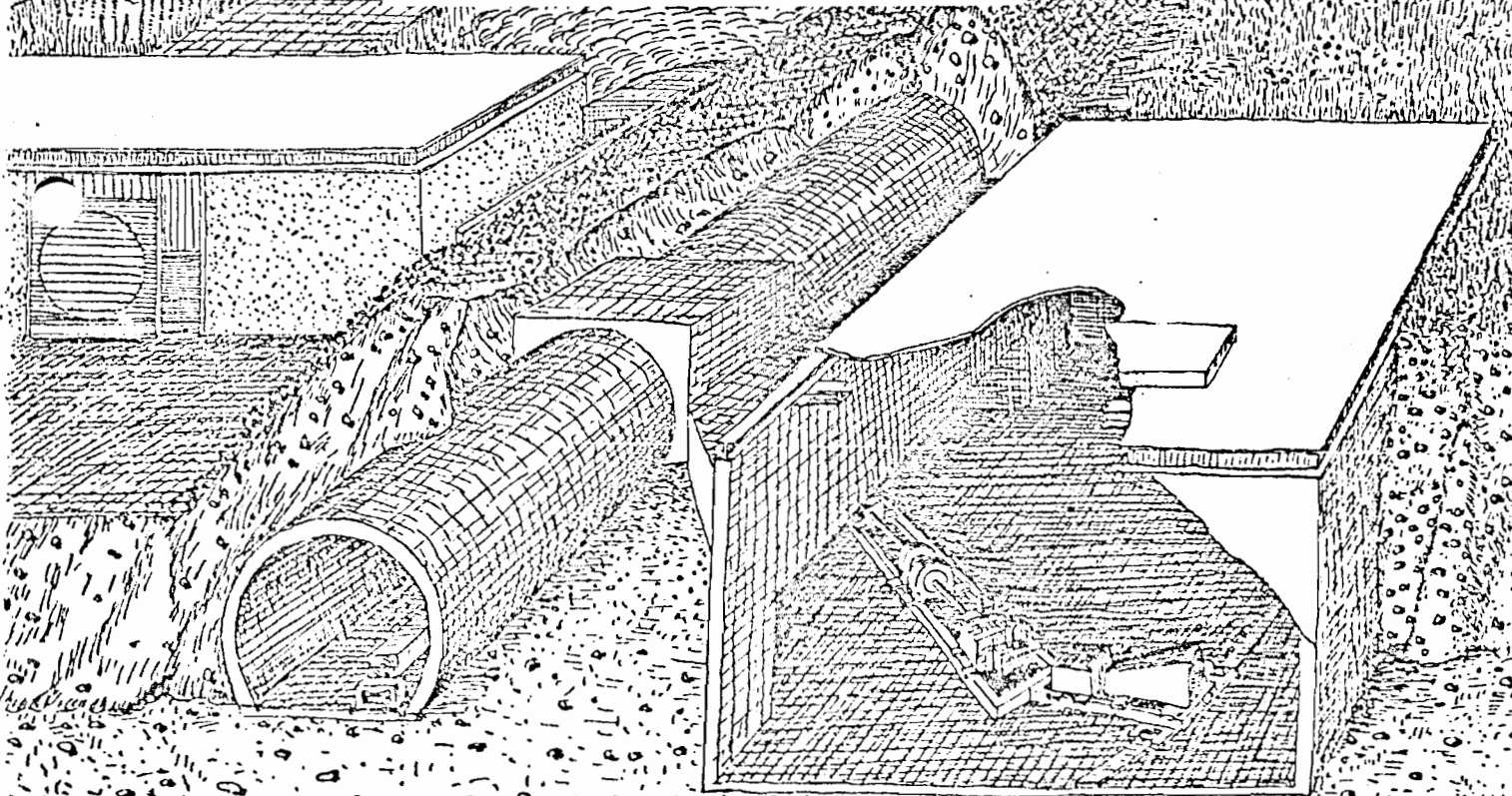


PRELIMINARY POLARIZATION RESULTS AT FERMILAB ENERGIES

M.D. Corcoran, S.E. Ems, F. Fredericksen, S.W. Gray,
B. Martin, H.A. Neal, H.O. Ogren, D.R. Rust, J.R. Sauer, P. Smith

Department of Physics
Indiana University
Bloomington, Indiana 47401



Preliminary Polarization Results

at Fermilab Energies*

M.D. Corcoran, S.E. Ems, F. Fredericksen,
S.W. Gray, B. Martin, H.A. Neal, H.O. Ogren,
D.R. Rust, J.R. Sauer, and P. Smith

Department of Physics
Indiana University
Bloomington, IN 47401

Abstract:

This paper describes the jet target, the superconducting spectrometer and the polarimeter used to measure the recoil proton polarization in an Indiana University experiment at the Fermi National Accelerator Laboratory. Analysis procedures and data checks are explained and preliminary results are presented and compared with model predictions. The future plans of the experiment are also discussed.

*Work supported by U.S. Energy Research and Development Administration under Contract E(11-1)2009, Task A. Paper submitted to the Coral Gables Orbis Scientiae January, 1977.

Introduction:

Recently there have been experimental and theoretical indications that the polarization in pp elastic scattering may be surprisingly large at high energies at certain t values. The ISR measurements of the dip in the differential cross section (Ref. 1) suggest the possibility of large polarizations. The Pumplin-Kane (Ref. 2) model predicts that polarization effects will persist to very high energies. Polarization measurements at Serpukhov suggest large polarizations at $|t| \geq .7$ at 45 GeV/c (Ref. 3).

Our group has undertaken a program to measure the polarization of protons from both elastic and inclusive interactions in the Internal Target Area (ITA) at Fermilab. Together with the ITA staff and another group of experimenters (E198A, a University of Rochester, Rutgers University, and Imperial College of London collaboration) we constructed a spectrometer to detect pp elastic scattering. To this we appended a polarimeter designed to measure recoil proton polarizations with a minimum of systematic bias.

Jet Target:

The target utilized was a hydrogen gas jet pumped by large diffusion pumps (see Figure 1). Hydrogen gas at ~ 10 atmospheres pressure is ejected from a 3 mil nozzle through the circulating Fermilab beam. Most of the gas is caught by a special mylar cone and directed into a 1 m^3 buffer volume. This large volume reduces the pressure to a level which the two ten inch diffusion pumps can handle. Two more ten inch pumps are on the main vacuum chamber. Other pumps up and downstream minimize the spread of the pressure

bump. To further limit the amount of gas introduced into the main ring the jet itself is pumped from behind the nozzle after the pulse is over.

The jet has a density of $\sim .5 \times 10^{-7} \text{ g/cm}^3$ and a width of $\sim 6 \text{ mm}$ FWHM. Typically we used three 100 ms jets during each ramp. The limit in integrated luminosity was set by the maximum permissible beam loss in the Internal Target Area.

Spectrometer:

The spectrometer uses a superconducting quadrupole doublet and a superconducting dipole to identify elastic protons produced in beam-jet interactions (see Figure 2). The quadrupoles are tuned to act as a field lens and to focus protons with the same production angle to a point; this allows the measurement of the angle with a single position measurement. The chamber unit used to measure the production angle θ has two x planes with 1.3 mm spacing (staggered by one half wire) and a single y plane. A similar chamber assembly about 1 meter downstream permits a momentum dependent correction to the angle measurement and serves as the first point in the momentum determination. Two more modules are mounted on each side of the dipole. The final two chambers are 15° tilted u, v chambers with 2 mm wire spacing. Two trigger counters and 3 hodoscopes are placed between the first 2 chamber modules. Another trigger counter and another hodoscope are at the end of the spectrometer.

Two experiments can read the chambers asynchronously. Our amplifiers look at the output of the spectrometer amplifiers and treat the signals similarly to the signals from our own polarimeter chambers. The spectrometer acceptance

is ~ 10 mr horizontally by ~ 40 mr vertically. The momentum bite is $\sim \pm 5\%$. The momentum resolution is presently approximately 1%. The missing mass resolution is 100 MeV (FWHM) at 100 GeV/c. At $t = -.3$ (GeV/c)² and $p_{\text{LAB}} < 100$ GeV/c the spectrometer produces a beam of elastically scattered recoil protons with essentially negligible inelastic contamination. A typical missing mass distribution for $t = -.8$ (GeV/c)² at $p_{\text{LAB}} = 40$ GeV/c is shown in Figure 3.

Polarimeter:

The polarimeter consists of proportional chamber telescopes (both x and y) on each side of a carbon re-scattering target (shown in Figure 4). The carbon analyzer has an effective analyzing power between .2 and .3 for accepted projected scattering angles between 6° and 22° . The analyzer was calibrated in the Argonne ZGS polarized proton beam. The x and y hodoscopes are used to resolve track ambiguities. Range counters with variable absorbers can be used to "enrich" the elasticity of the double scatters and improve the analyzing power. A key feature is the polarimeter's ability to rotate about its axis allowing left and right to be interchanged; all first order instrumental asymmetries then average to zero.

A second important feature of the polarimeter is a hardwired computer. Since only a few percent of the elastic scatters detected by the spectrometer actually interact in the carbon target, most fast logic triggers are uninteresting. The polarimeter computer uses information from the proportional chambers before they are read out to enrich the fraction of recorded usable double scatters by a

factor of 20 - 80. It first checks that there is an incident track in each view (x and y) approximately normal to the polarimeter. Next it searches for a companion track in the chambers after the carbon target which could signal a simple straight-through. It also searches for a companion track in the rear chambers which looks like a true scatter. The choice, tolerances, and specifications of the tests appropriate for each recoil momentum and each thickness of carbon target used can be remotely selected from the electronics trailer. An illustration of the effectiveness of the polarimeter computer in enhancing the recorded number of useful double scatters is shown in Figure 5.

Analysis Procedure:

In the polarization analysis only those events were retained which reconstructed in both views and which had consistent chamber and hodoscope trajectory information. Cuts were placed on the re-scattering vertex to ensure that all events utilized in the polarization determination did indeed scatter in the carbon target. A typical vertex distribution in the coordinate along the polarimeter axis is shown in Figure 6. Only double scatters within the projected angle range $6^\circ - 22^\circ$ were utilized. This was done to maximize the net analyzing power and analyzing efficiency and to correspond to the experimental conditions in the calibration measurements.

To minimize the effects of instrumental asymmetries several precautions were taken. The most important protection against biases came from the averaging out of first order instrumental asymmetries by rotating the entire polarimeter by 180° about its axis. This flipping of the polarimeter about the

nominal recoil beam centroid permitted "left" and "right" to be effectively interchanged so that effects due to asymmetric chamber or counter inefficiencies are cancelled when the results from the two supplementary orientations are averaged. The relative polarimeter chamber alignment was monitored at frequent intervals by analyzing straight-through events. The efficiencies of all chambers and hodoscopes were continually monitored as a function of position by using several independent schemes.

Other checks involved a measurement of the up-down instrumental asymmetry with the polarimeter at its 0° , 90° , and 180° azimuthal orientations and the measurement of the asymmetry resulting from the double scattering of pions. In all cases the results of these tests were consistent with the polarimeter having a left-right bias less than $\Delta\epsilon = .01$. The effect of this bias on results obtained by averaging data from the 0° and 180° orientations is found to be consistent with zero ($\Delta\epsilon < .001$). Furthermore, the polarimeter was used to measure the polarization at $t = -.3 \text{ (GeV/c)}^2$ near 17 GeV c where the polarization is well-known from previous measurements. This check was successful and illustrates the polarimeter's capability to detect finite proton polarizations.

The polarization P is determined from the relations

$$\epsilon \equiv \frac{L - R}{L + R} ,$$

$$P = \frac{1}{A} \epsilon , \text{ where}$$

L and R are the number of double scatters in the left and right angular regions corresponding to horizontally projected angles between 6° and 22° . A is the

analyzing power which was determined in a calibration experiment in the ZGS polarized beam for a large range of proton energies (Ref. 4).

Results:

Preliminary results from this experiment at $t = -.3$ and $t = -.8$ $(\text{GeV}/c)^2$ at several s values are given in Figures 7, 8 along with other data at these t values. At $t = -.3$ $(\text{GeV}/c)^2$ the polarization is seen to drop from a very large value of $\sim 35\%$ at $s = 6$ GeV^2 to $\sim 1\%$ at $s = 100$ GeV^2 . At $t = -.8$ $(\text{GeV}/c)^2$, however, a significant negative polarization appears to develop near $s = 100$ GeV^2 . This sizeable negative polarization which was also suggested in earlier Serpukhov data at $p_{\text{LAB}} = 45$ GeV/c , is in contrast to the small positive value of the polarization at this t value at all $p_{\text{LAB}} < 20$ GeV/c . Theories must confront the question of why such spin effects exist at high energies. It is of interest to note that the small positive polarization at small $|t|$ ($|t| < .4$ $(\text{GeV}/c)^2$) and the rather large negative polarizations for $|t|$ in the vicinity of $.7 - 1.0$ $(\text{GeV}/c)^2$ is a prediction of the Pomplin - Kane model.² The agreement of a prediction of this model with the fixed t data is illustrated in Figures 7, 8. The model's predictions arise from an exploration of the consequences of the Pomeron having quantum numbers different from the vacuum. The pursuit of the implications of this fundamental idea seems to be absolutely essential.

Future Plans:

Our present plans are to explore the development in energy of polarization effects near $t = -.8$ $(\text{GeV}/c)^2$. The experiment is particularly well-adapted to fixed t studies since the analyzing power and acceptance are nearly independent

of s . Later we plan to complete s sweeps of the polarization at other t values in the region $.3 < |t| < 1.0 \text{ (GeV/c)}^2$. We also plan some less precise explorations near the dip in the elastic differential cross section where effects at the 30 - 50% level are predicted by some models. In addition, we plan to study the polarization of protons produced inclusively over a wide range of s .

Acknowledgements

We wish to thank the Fermilab Internal Target Group for their role in building the spectrometer room, the spectrometer itself, and the jet target. We also wish to acknowledge the E-198 experimenters from the University of Rochester, Rutgers University, and the Imperial College of London for their contributions to the spectrometer effort and for the use of some of their equipment.

References

1. A. Bohm et al., Phys. Letters 49 B, 491 (1974).
2. J. Pumplin and G. L. Kane, Phys. Rev. D 11, 1183 (1975).
3. A. Gaidot et al., Phys. Letters 61 B, 103 (1976).
4. G. W. Bryant, H. A. Neal, D. R. Rust, "Proton-Carbon Analyzing Power Measurements for Proton Kinetic Energies between .150 GeV and .440 GeV", Indiana University Internal Report COO-2009-102.

Figure Captions

- Fig. 1 Illustration of hydrogen gas jet.
- Fig. 2 Layout of the internal target superconduction spectrometer. Q_1 and Q_2 are quadrupole magnets. SPC1-11 are multiwire proportional chambers. H1-4 are hodoscopes and S1-4 are trigger counters.
- Fig. 3 Missing mass distribution at $t = -.8 \text{ (GeV/c)}^2$.
- Fig. 4 Layout of polarimeter. T_1 and T_2 are trigger counters. PC1-4 are multiwire proportional chambers. HX and HY are hodoscopes. R1-R3 form a range telescope.
- Fig. 5 Illustration of the effectiveness of the polarimeter computer in suppressing small angle double scatters.
- Fig. 6 Double scattering vertex distribution along polarimeter axis.
- Fig. 7 Preliminary polarization results at $t = -.3 \text{ (GeV/c)}^2$. The curve shown is a prediction of the model in Ref. 2.
- Fig. 8 Preliminary polarization results at $t = -.8 \text{ (GeV/c)}^2$. The curve shown is a prediction of the model in Ref. 2.

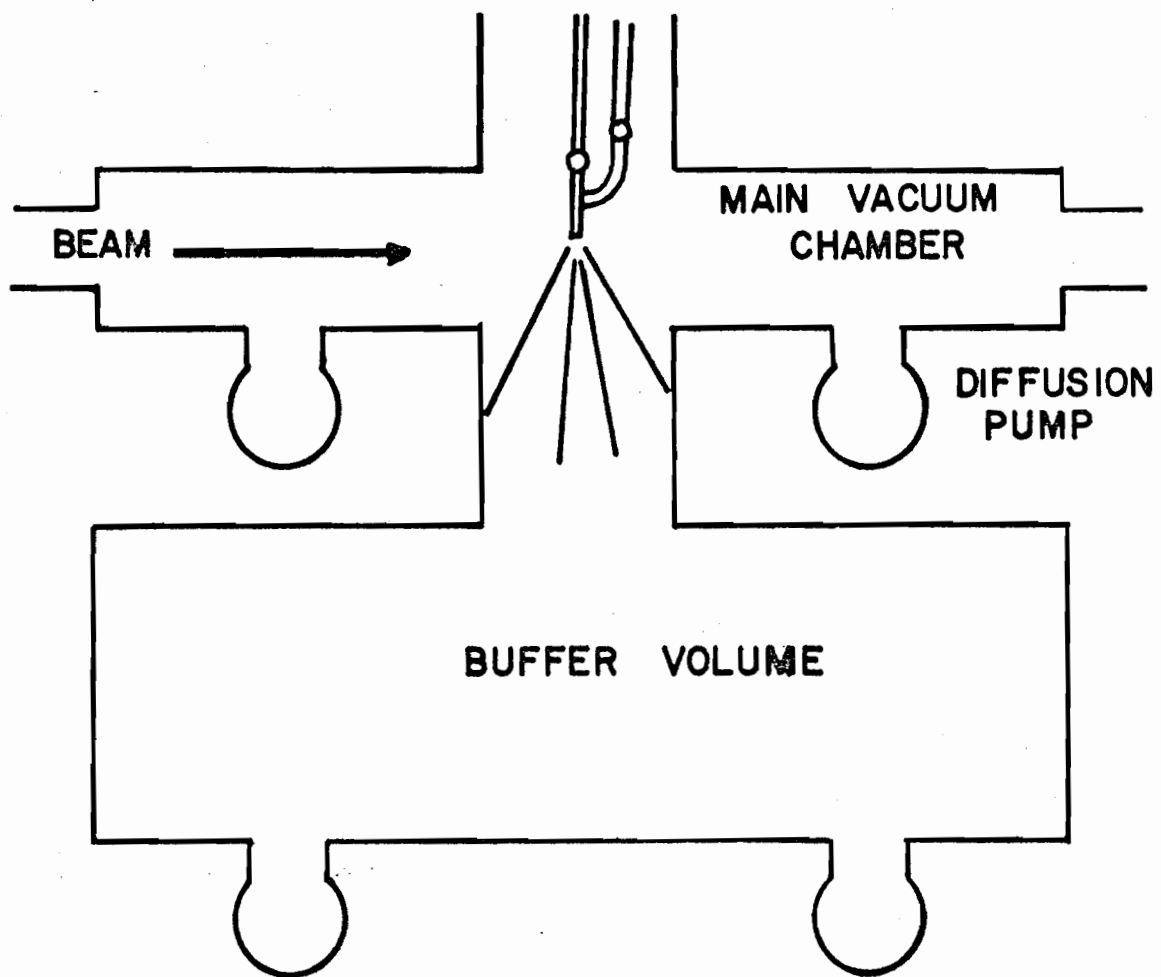
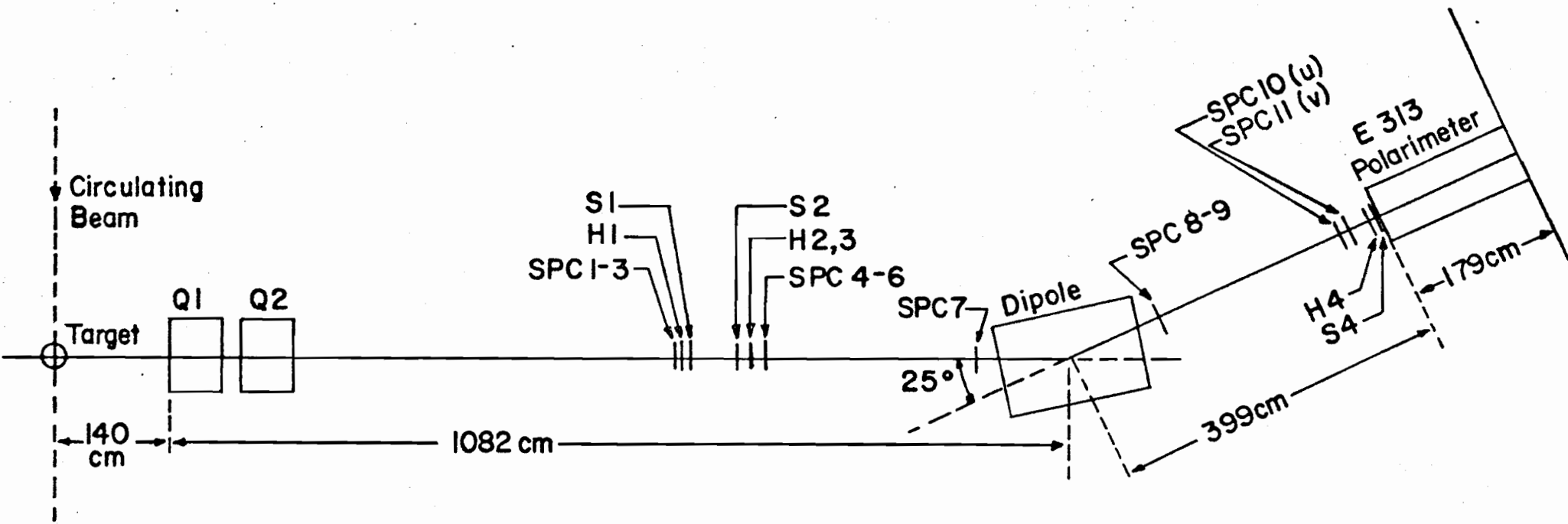


FIGURE I



Scale: 70:1

INTERNAL TARGET SPECTROMETER

FIGURE 2

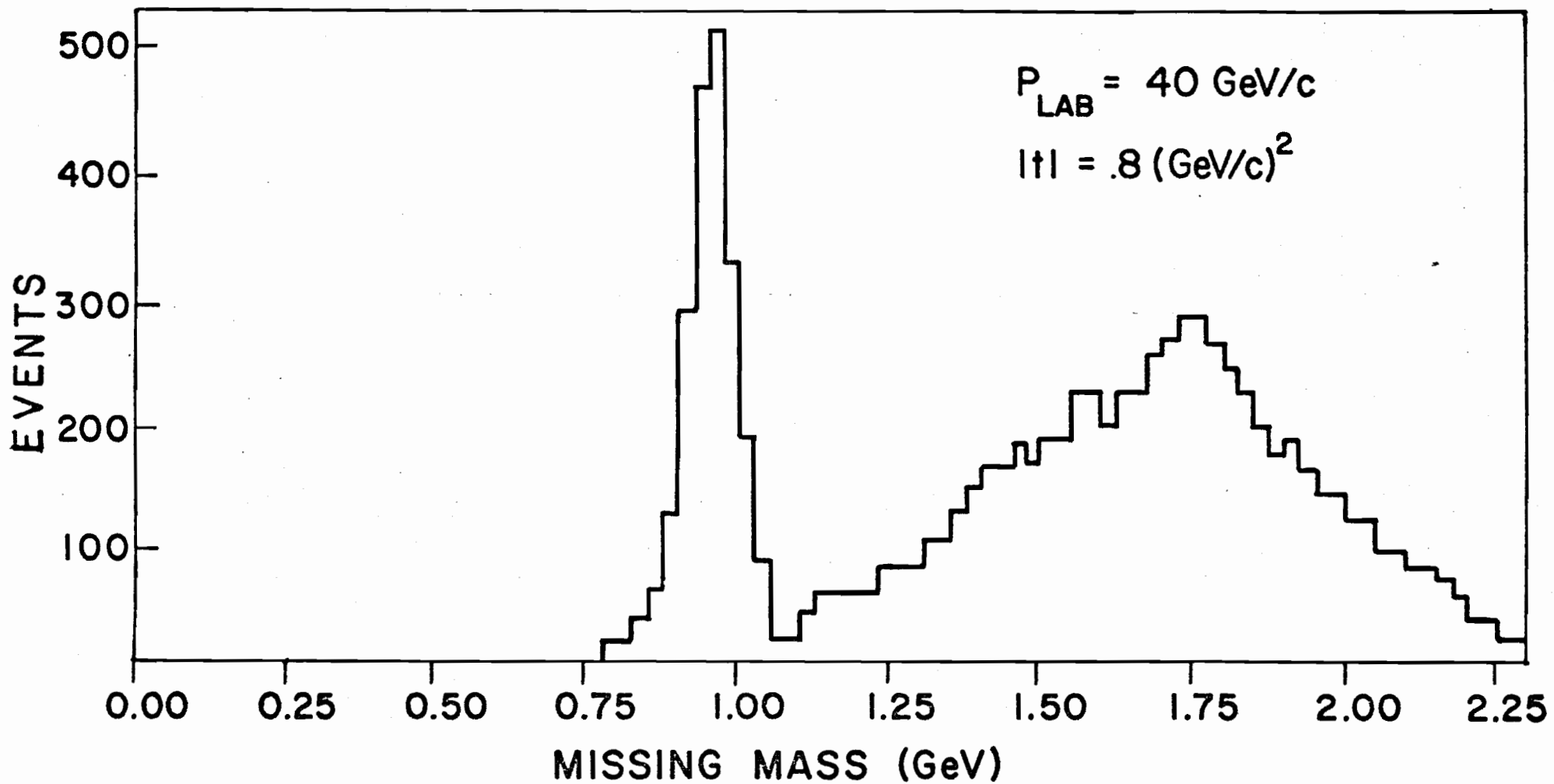
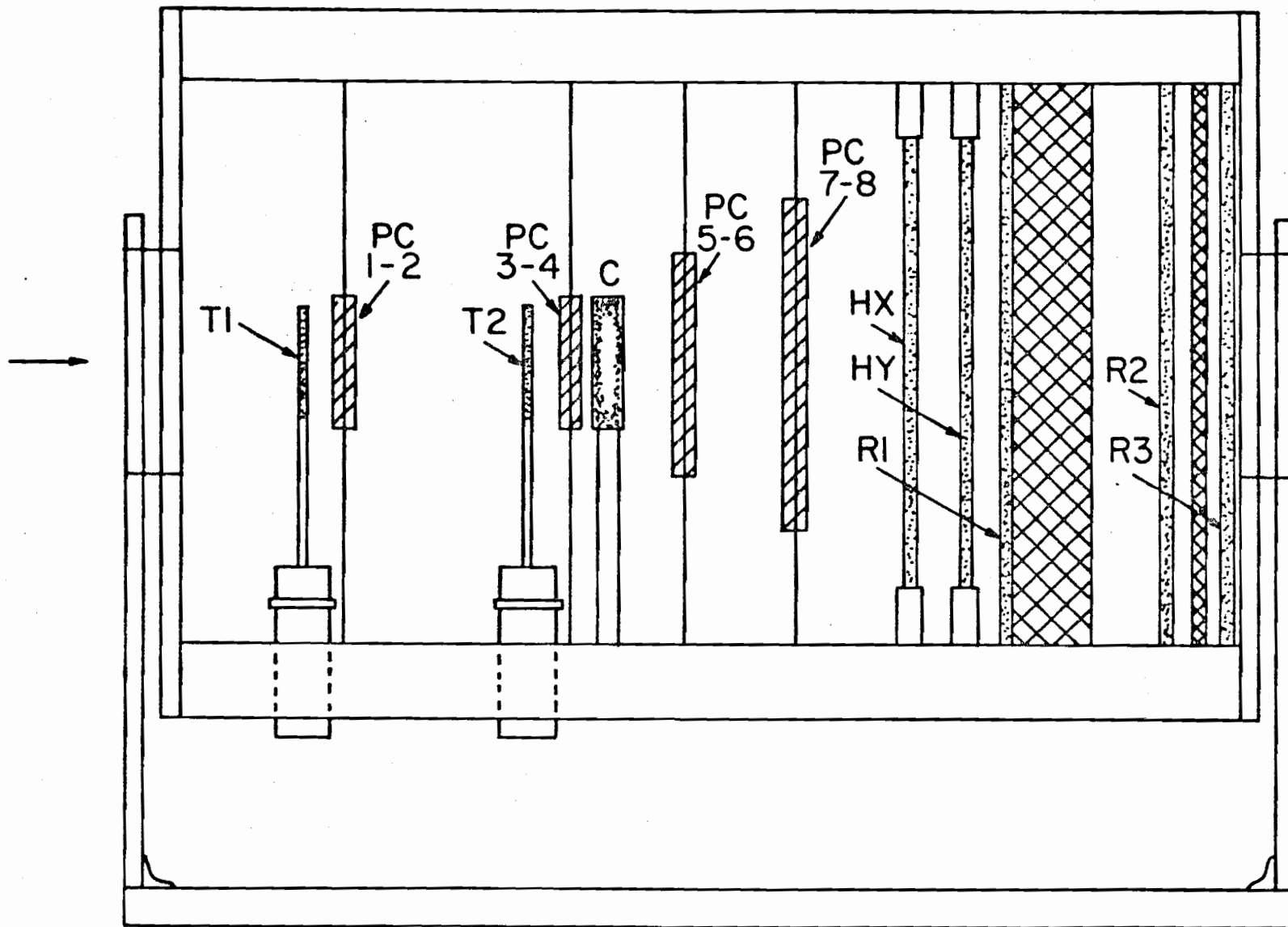


FIGURE 3



POLARIMETER LAYOUT

scale: 8:1




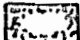
-  proportional chambers
-  range steel
-  scintillation counters
-  carbon block

FIGURE 4

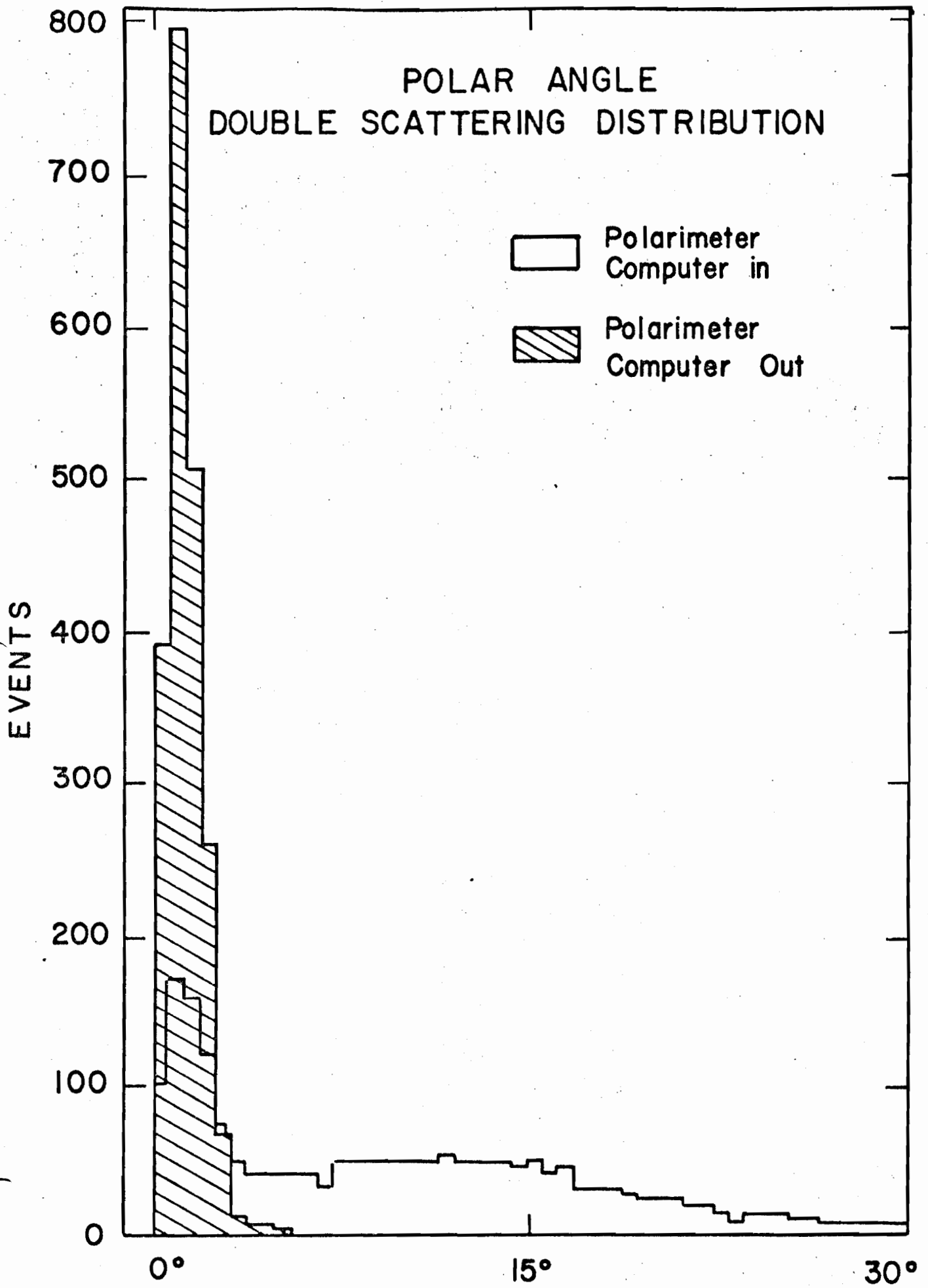


FIGURE 5

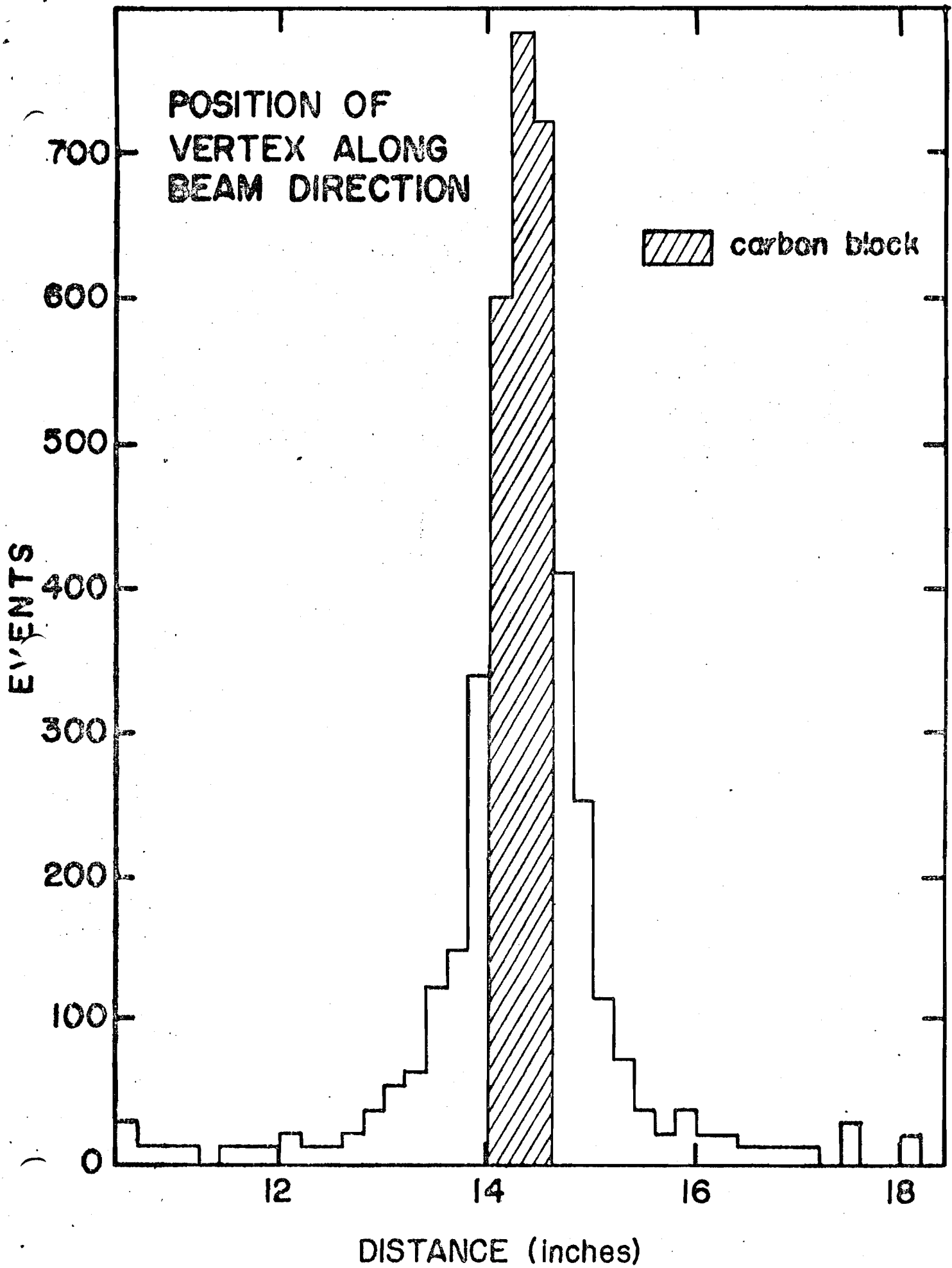
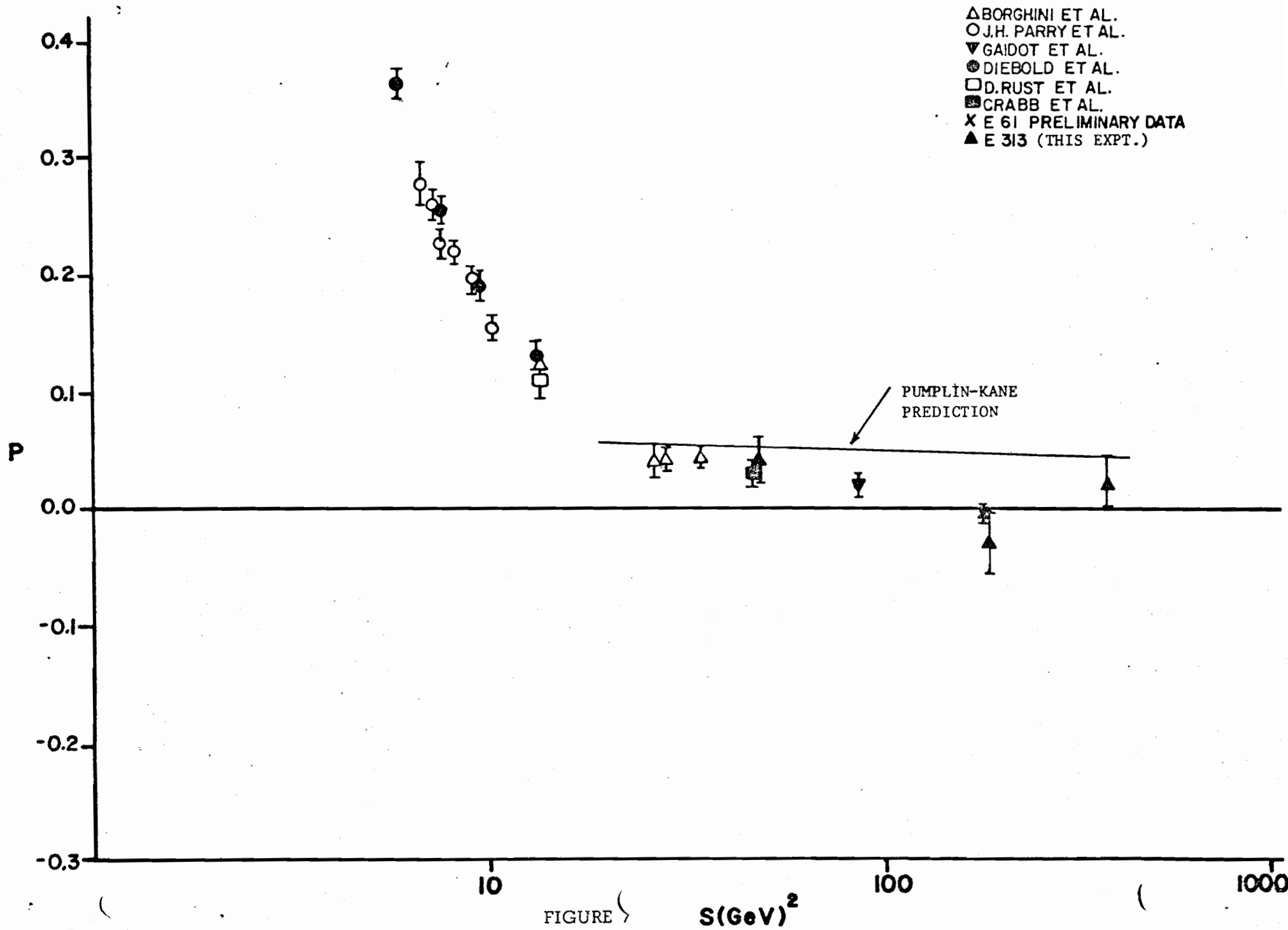


FIGURE 6

POLARIZATION IN PP ELASTIC SCATTERING AT $|t| = .3 (\text{GeV}/c)^2$



FIGURE

$S(\text{GeV})^2$

POLARIZATION IN PP ELASTIC SCATTERING AT $|t| = .8 \text{ (GeV/c)}^2$

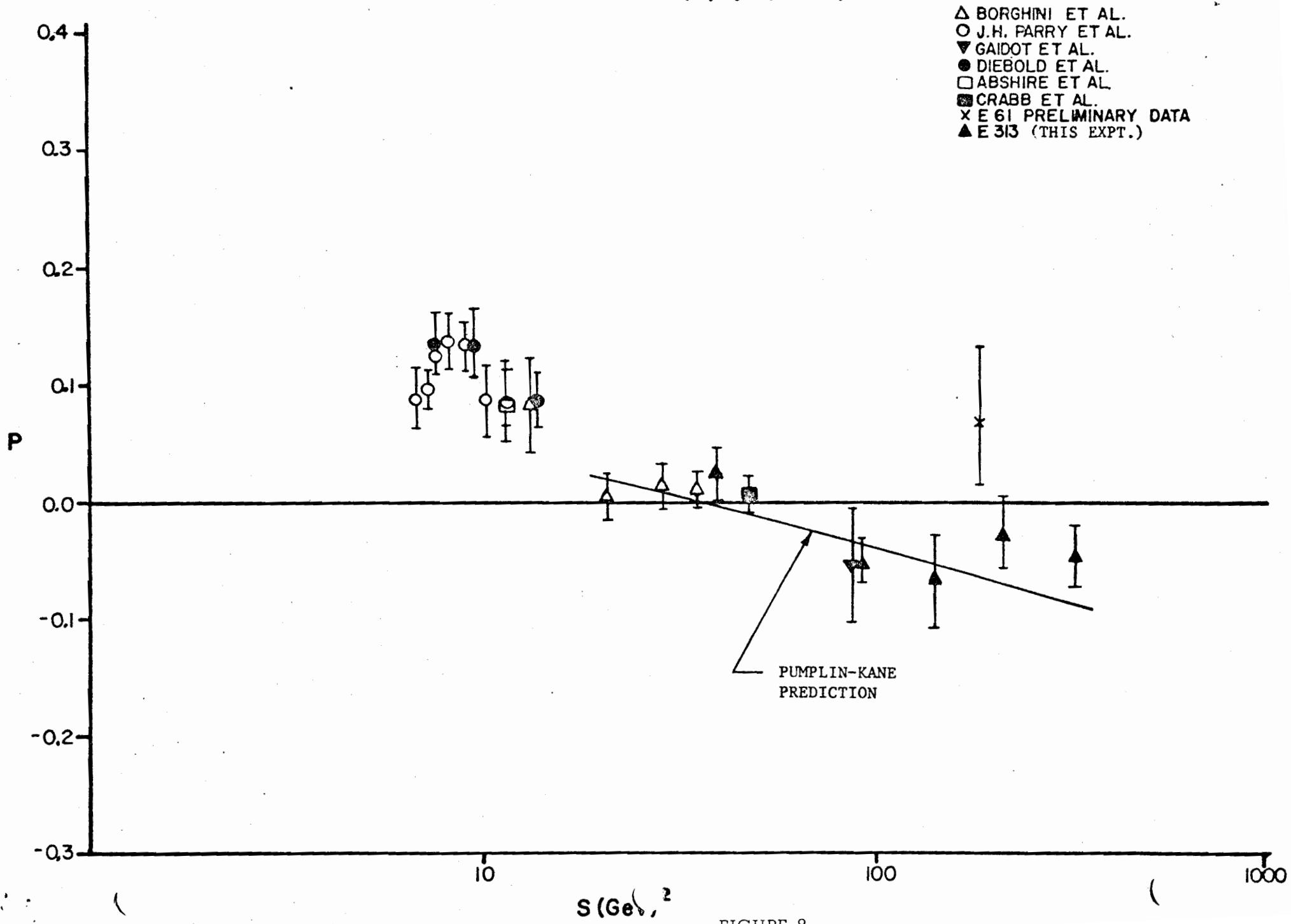


FIGURE 8